# Detection and Characterization of Intrinsic Symmetry of 3D Shapes

Anirban Mukhopadhyay† Suchendra M. Bhandarkar‡ Fatih Porikli*
†Department of Visual Data Analysis, Zuse Institute Berlin, Berlin, Germany
‡Department of Computer Science, The University of Georgia, Athens, Georgia, USA
*College of Engineering & Computer Science, Australian National University, Canberra, Australia
Emails: {anirban.akash@gmail.com suchi@cs.uga.edu fatih.porikli@anu.edu.au}

***Abstract*—A comprehensive framework for detection and characterization of partial intrinsic symmetry over 3D shapes is proposed. To identify prominent symmetric regions which overlap in space and vary in form, the proposed framework is decoupled into a *Correspondence Space Voting* (CSV) procedure followed by a *Transformation Space Mapping* (TSM) procedure. In the CSV procedure, significant symmetries are first detected by identifying surface point pairs on the input shape that exhibit *local* similarity in terms of their intrinsic geometry while simultaneously maintaining an intrinsic distance structure at a *global* level. To allow detection of potentially overlapping symmetric shape regions, a *global intrinsic distance-based voting* scheme is employed to ensure the inclusion of only those point pairs that exhibit significant intrinsic symmetry. In the TSM procedure, the *Functional Map* framework is employed to generate the final map of symmetries between point pairs. The TSM procedure ensures the retrieval of the underlying dense correspondence map throughout the 3D shape that follows a particular symmetry. The TSM procedure is also shown to result in the formulation of a *metric symmetry space* where each point in the space represents a specific symmetry transformation and the distance between points represents the complexity between the corresponding transformations. Experimental results show that the proposed framework can successfully analyze complex 3D shapes that possess rich symmetries.**

## I. Introduction

The detection and characterization of shape symmetry has attracted much recent attention within the computer graphics and computer vision communities [12]. Most of the existing literature has focused on the detection of *extrinsic* symmetries, a popular approach being transformation space voting [11]. However, there has been steadily growing interest in detection and characterization of *intrinsic* symmetries; especially *global* symmetries [9], [13].

Symmetry can be considered as a *distance-preserving* transformation. For a symmetry transformation $T$, the distance between two points $p$ and $q$ on the surface of a 3D shape is equal to the distance between the corresponding transformed surface points $T(p)$ and $T(q)$. In the case of *extrinsic* symmetry, the *Euclidean* distance measure is used, whereas in the case of *intrinsic* symmetry, intrinsic distance measures such as, the *geodesic distance measure* (GDM) or the *biharmonic distance measure* (BDM) are used. Detection of *overlapping* intrinsic symmetry is a more challenging problem due to the significantly larger search space involved in the detection of symmetric regions (when compared to global symmetry analysis) and in the determination of symmetry revealing transforms (when compared to extrinsic symmetry detection) [11], [12]. The problem of detection and characterization of overlapping intrinsic symmetry is more general, since the extrinsic symmetry detection problem can be considered a special case of overlapping intrinsic symmetry detection [12].

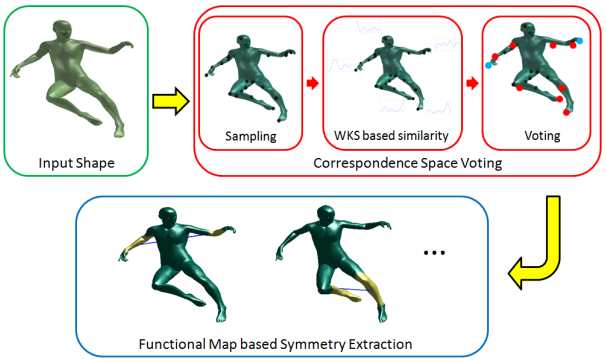


Fig. 1. Overview of the proposed symmetry detection and characterization framework.

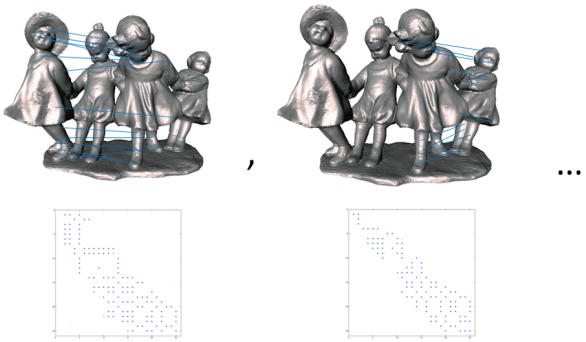


Fig. 2. Symmetry extraction in functional space. The top row depicts two significant symmetry transformations along with a few representative point correspondences. The corresponding functional map matrices are shown in the bottom row.

An intrinsic symmetry over a 3D shape is a subregion with associated *self-homeomorphisms* that preserve all pairwise intrinsic distances [12]. Complex shapes often exhibit multiple symmetries that overlap spatially and vary in visual appearance as depicted in Fig. 2. Analysis of overlapping symmetry poses significant challenges.

The key idea behind the proposed scheme for intrinsic

symmetry detection and characterization is to approach the problem from a shape correspondence perspective and generate the transformation map which can be further used to describe the symmetry space. To this end, given a 3D shape, approximated by a triangular mesh, as input, we perform two stages of processing. In the first stage, representative symmetric point pairs are identified based on their local geometry and a global distance representation. In the second stage, the original transformation is retrieved as a *functional map* to facilitate further characterization of the underlying symmetry. The detected intrinsic symmetries are representative of the 3D shape and the corresponding functional matrices exhibit a high degree of *diagonality*, as shown in Fig. 2.

The primary contributions of our paper are as follows:

(1) We exploit the functional map representation in conjunction with the Correspondence Space Voting (CSV) procedure of Xu et al. [23]. In Xu et al. [23], the CSV procedure is followed by a computationally complex optimization step for symmetry detection that comprises of a two-stage clustering procedure. The proposed algorithm, in contrast, is based on the detection of a few initial symmetric candidates followed by a computationally efficient generalization procedure for overall symmetry detection that is based on the functional map representation and the solving of a system of linear equations.

(2) We provide robust and meaningful characterization of the symmetry transformation by formulating a *symmetry space* which allows one to *quantitatively* distinguish between instances of simple and complex intrinsic symmetry. To the best of our knowledge, such quantitative characterization of symmetry has not been attempted in the published literature.

## II. Related Work

Since an *exhaustive* exposition of the state of the art in symmetry detection is beyond the scope of this paper, we restrict our discussion to existing works that are most closely related to the proposed approach, and direct the interested reader to the comprehensive survey by Mitra et. al. [12]. Most existing approaches to intrinsic symmetry detection based on region growing [22], partial matching [20], and symmetry correspondence [9] cannot extract physically overlapping symmetries. Recent algorithms for detection of approximate and partial extrinsic symmetries are based on clustering of *votes* in a parameterized *transformation space* [8], [11]. Xu et al. [23] let surface point pairs vote for their partial intrinsic symmetry and subsequently perform intrinsic symmetry grouping. However, their method cannot retrieve the final symmetry map which makes characterization of the specific intrinsic symmetry very difficult. Moreover, the aforementioned methods are ineffective at finding correspondences between points in complex symmetry orbits that are spread across multiple distinct clusters in the transformation space. They also suffer from the curse of dimensionality in that the voting procedure in high-dimensional transformation space becomes increasing intractable when dealing with complex symmetries.

Another class of symmetry detection techniques characterizes shape representations based on the extent of symmetry displayed by an object with respect to multiple transformations [7], [17], [25]. Although these shape representations provide a measure of symmetry for a regularly sampled set of transformations within a group, they are practical only for transformation groups of low dimensionality. Lipman et al. [9] have proposed an eigenanalysis technique for symmetry detection that relies on spectral clustering. Xu et al. [23] have extended the eigenanalysis approach to distinguish between scale determination and symmetry detection by incorporating the concept of global intrinsic distance-based symmetry support accompanied by a two-stage spectral clustering procedure. However, their two-stage spectral clustering procedure [23] is computationally complex and further processing of the detected symmetries, which are represented as point pairs, is extremely inefficient.

## III. Theoretical Framework

The proposed algorithm for symmetry detection and characterization is decoupled into two stages termed as *Correspondence Space Voting* (CSV) and *Transformation Space Mapping* (TSM) or *Functional Map Retrieval* (FMR). The terms TSM and FMR are used interchangeably in this paper. For CSV, a joint criterion that combines local intrinsic surface geometry and global intrinsic distance-based symmetry is proposed, and is shown to result in a provably necessary condition for intrinsic symmetry. Although the CSV procedure is inspired by the work of Xu et al. [23], we have bypassed the two computationally intensive procedures in their scheme, i.e., spectral clustering and all-pairs geodesic distance computation [23], to improve significantly the running time of the proposed CSV procedure. Moreover, our incorporation of the TSM or FMR procedure in symmetry detection is novel in that it not only provides a *concise description* of the underlying symmetry transformation, but also enables its *formal characterization*. We propose a formal TSM-based scheme for characterization of the complexity of the detected symmetries and also demonstrate its effectiveness.

The CSV procedure is used as an initialization step in the proposed algorithm. Following the initial detection of good symmetry correspondences using CSV, we retrieve the symmetry transformation map using the functional map framework. The generalization of symmetry detection over the entire surface is performed by solving a system of linear equations which not only returns the underlying symmetry transformation map, but also ensures the scalability of symmetry detection with respect to the number of surface points. The intrinsic symmetry criterion ensures that the retrieved functional matrix exhibits *diagonality*. The inner product of the functional matrix with a suitably formulated cost matrix is shown to provide a *quantitative* measure of the complexity of the detected symmetry. In the following subsections, we summarize some previously formulated concepts, tools and techniques that are used in the proposed algorithm.

### A. Biharmonic Distance Measure

An intrinsic distance measure between pairs of points on a 3D surface needs to be a metric, smooth, locally isotropic, globally shape-aware, isometry invariant, insensitive to noise and small topological changes, parameter-free, and practical to compute on a discrete mesh. While most existing intrinsic distance measures do not possess all the above properties, the *biharmonic distance measure* (BDM) is one of the few in the published literature that does [9]. The BDM kernel is based on the Green's function of the biharmonic differential equation. The (squared) biharmonic distance between two points $x$ and $y$ can be defined using the eigenvectors ($\phi_k$) and eigenvalues ($\lambda_k$) of the Laplace-Beltrami operator [9] as follows: $d_M(x,y)^2 = \sum_{k=1}^{\infty} \frac{(\phi_k(x) - \phi_k(y))^2}{\lambda_k^2}$. The BDM captures the rate of decay of the normalized eigenvalues $\lambda_k$ of the Laplace-Beltrami operator; if the decay is too slow, it produces a logarithmic singularity along the diagonal of the Green's function [24]. Alternatively, too fast a decay basically ignores the eigenvectors associated with higher frequencies, resulting in the BDM being global in nature (i.e., the local surface details are ignored). Lipman *et al.* [10] have demonstrated that quadratic normalization provides a good balance between the two extremes.

### B. Wave Kernel Signature

The Wave Kernel Signature (WKS) of a surface point $x$ is a descriptor that evaluates the probability of a quantum particle with a certain energy distribution to be located at point $x$. If the quantum particle has an initial energy distributed around some nominal energy with a probability density function $f(e)$, then the solution of the Schrodinger equation can then be expressed in the spectral domain as: $\psi(x,t) = \sum_{k>=1} e^{ie_k t} f(e_k)\phi_k(x)$. Aubry et al. [1] consider a family of log-normal energy distributions centered around some mean log energy, i.e., $\log e$, with variance $\sigma^2$. For a family of energy distributions, each point $x$ on the surface is associated with a WKS of the form: $p(x) = (p_{e_1}(x), \ldots, p_{e_n}(x))^T$ where $p_{e_i}(x)$ is the probability of measuring a quantum particle with the initial energy distribution $e_i(x)$ at point $x$. The WKS can be shown to exhibit a band-pass characteristic which reduces the influence of low frequencies and allows for better separation of frequency bands across the descriptor dimensions.

### C. Functional Map

A functional map [15] is a novel approach for inference and manipulation of maps between 3D shapes. It provides an elegant means for avoiding the direct representation of correspondences as mappings between shapes. Rather than plotting the corresponding points on the 3D shapes, the mappings between functions defined on the 3D shapes are considered. This notion of correspondence generalizes the standard point-to-point map since every point-wise correspondence induces a mapping between function spaces [15].

Ovsjanikov et al. [15] have noted that when two shapes $X$ and $Y$ are related by a bijective correspondence $t : X \to Y$, then for any real function $f : X \to \mathbb{R}$, one can construct a corresponding function $g : Y \to \mathbb{R}$ as $g : f \circ t^{-1}$. Equipping $X$ and $Y$ with harmonic bases, $\{\phi_i\}_{i\geq 1}$ and $\{\psi_j\}_{j\geq 1}$, respectively, one can represent a function $f : X \to \mathbb{R}$ using the set of (generalized) Fourier coefficients $\{a_i\}_{i\geq 1}$ as $f = \sum_{i\geq 1} a_i\phi_i$. Translating this representation into the other harmonic basis $\{\psi_j\}_{j\geq 1}$, one obtains a simple representation of the correspondence between the shapes given by $T(f) = \sum_{i,j\geq 1} a_i c_{ij} \psi_j$ where $c_{ij}$ are Fourier coefficients of the basis functions of $X$ expressed in the basis of $Y$, defined as $T(\phi_i) = \sum_{i,j\geq 1} c_{ij}\psi_j$. The correspondence $t$ between the shapes can thus be approximated using $k$ basis functions and encoded using a $k \times k$ matrix $C = (c_{ij})$ of these Fourier coefficients, referred to as the functional matrix. The functional matrix $C$ has a diagonal structure if the harmonic bases $\{\phi_i\}_{i\geq 1}$ and $\{\psi_j\}_{j\geq 1}$ are *compatible*, i.e., if the bijective correspondence $t$ is isometry preserving.

### D. The Proposed Algorithm - Input and Output

The input to the algorithm is a *3D shape* that is represented by a compact, connected 2-manifold, $M$, with or without a boundary, i.e., $M \to \mathbb{R}^3$. Distances on the manifold $M$ are expressed in terms of an intrinsic distance measure such as the BDM. The BDM is used on account of its ease of computation and greater robustness to local surface perturbations when compared to the GDM [10]. We use the terms "intrinsic distance" and "biharmonic distance" interchangeably in this paper. Since a symmetry transformation is represented by a functional map, the output of the proposed algorithm consists of functional maps represented as matrices which can be regarded as a complete and compact description of all the overlapping intrinsic symmetries of the 3D shape.

### E. Definition of Intrinsic Symmetry

Given a compact connected 2-manifold $M$ without a boundary, we deem $M$ to be intrinsically symmetric if there exists a *homeomorphism* $T\colon M \to M$ on the manifold that preserves all intrinsic distances [19]. That is, $d_M(p,q) = d_M(T(p),T(q))\ \forall p,q \in M$, where $d_M(p,q)$ is the intrinsic distance between two points on the manifold. In this case, we call the mapping $T$ an intrinsic symmetry.

### F. Symmetry Criteria

We propose two simple criteria to test whether two surface point pairs $\{x,x'\}$ and $\{y,y'\}$ on the manifold $M$ potentially share the same intrinsic symmetry. The first is a *local intrinsic geometry criterion* that determines the symmetry potential of the two surface point pairs by comparing their corresponding WKS values: $\mathrm{WKS}(x,t) = \mathrm{WKS}(x',t)$ and $\mathrm{WKS}(y,t) = \mathrm{WKS}(y',t)\ \forall t \geq 0$, where $t$ is a scale parameter. The second is an *intrinsic distance criterion*: $d_M(x,y) = d_M(x',y')$ and $d_M(x,y') = d_M(y,x')$. The above two criteria are necessarily satisfied if the surface point pairs under consideration correspond to the same intrinsic symmetry [19], [23].

### G. Correspondence Space Voting (CSV)

The CSV procedure is used to initialize the proposed algorithm to ensure the success of the finally generated functional map. Our version of CSV, unlike [23], is performed in a reduced search space resulting from employing an efficient sampling strategy and the local geometric similarity criterion. Our CSV procedure comprises of the following three stages:
**Selection of Surface Points:** A subset $X$ consisting of $n$ sample surface points with adequate discriminative power is chosen from the input 3D shape surface using the *farthest point random sampling* strategy [6] thus ensuring a reduced search space for CSV. This strategy generates a set of points located mostly in the vicinity of the shape extrema. These points are then used in the subsequent generation of surface point pairs.
**Generation of Surface Point Pairs:** Surface point pairs are generated from the $n$ sample surface points in the chosen subset $X$ by computing the similarity of their WKS values as described in the local intrinsic geometry criterion. The surface point pairs that satisfy the local intrinsic geometry criterion to within a pre-specified threshold are considered *good voters* for inclusion in the subsequent global distance-based voting stage.
**Global Distance-based Voting:** A subset of symmetric point pairs is extracted from the set of *good voters* using a global distance-based voting procedure. A point pair in the set of *good voters* is deemed to be symmetric if it has sufficiently large global symmetry support, which is measured by the number of point pairs that satisfy the intrinsic distance criterion [23]. Our use of the BDM instead of the GDM (as in [23]) in the intrinsic distance criterion renders the voting procedure computationally more efficient and more robust to noise and small surface perturbations.

### H. Transformation Space Mapping and Symmetry Extraction

In the proposed algorithm, instead of comparing two different shapes, we compare two symmetric regions within the same shape. Based on the previously detected set of symmetric point pairs, we leverage the functional map representation for symmetry extraction. For each pair of symmetric points, we deem one point as the source and the other as the destination and choose a local region around each point. The ordering of the source and destination points within the pair is the same as the one originally chosen during CSV. The corresponding eigenbases for the points in the source and destination regions are computed. These eigenbases are ordered based on their mutual similarity and the final functional map for that particular symmetry is extracted. The functional map representation ensures that (a) the problem of symmetry extraction is tractable and, (b) the resulting symmetry can be represented, not by a large matrix of point correspondences, but rather as a more compact functional map which can be further manipulated.

## IV. Symmetry Characterization

Since the proposed CSV ensures that the point pairs used in functional map generation are intrinsically symmetric (to a reasonable extent), the resulting functional map is diagonal or close to diagonal [15]. Substantial deviation of the actual symmetry transformation from $\epsilon$-isometric deformation results in a more densely populated functional matrix $C$. The degree of off-diagonality of $C$ corresponds to the complexity of the symmetry transformation, i.e., more non-zero off-diagonal elements in $C$ implies a more complex symmetry transformation [18]. We formulate a weight matrix $W$ of the same dimensions as $C$ where the weight values are assigned based on an *inverted* Gaussian model, i.e., $W$: $w_{i,j} = 1 - \exp(-d_{i,j}^2)$ where $d_{i,j}$ is the distance of the $(i,j)^{th}$ element of $W$ from the matrix diagonal. Thus zero weights are assigned to the diagonal elements of $W$ whereas the off-diagonal weight values are an increasing function of their distance from the principal diagonal of $W$.

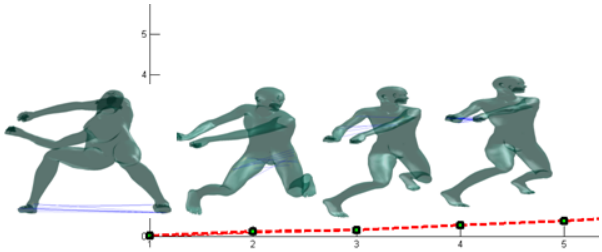


Fig. 3. The complexity of the symmetry transformation is characterized by the weight matrix $W$ and represented in the increasing order of the value of the inner product of $W$ and $C$.

The complexity of the symmetry transformation is captured by the inner product of $C$ and $W$ given by $\sum_i \sum_j w_{i,j} c_{i,j} = \sum_i \sum_j m_{i,j}$ which is a measure of the diagonality of $C$. The inner product allows each symmetry transformation to be represented as a point in the symmetry space with a value given by the inner product of the $C$ and $W$. The Euclidean distance between the points in the 1D symmetry space represents the complexity distance between the corresponding symmetry transformations (Fig. 3). The symmetry space can be shown to be a metric space because all the primary properties of a distance metric are preserved, i.e., non-negative definiteness, symmetry and triangle inequality. This also makes it possible to cluster the points in the 1D symmetry space to identify potentially similar intrinsic symmetries.

## V. Experimental Results

We present the results obtained by the proposed intrinsic symmetry detection algorithm on various 3D shapes from the *Non-rigid World* dataset [2] and compare them with results obtained from the most closely related approaches [9], [23]. We use the *cotangent* (COT) scheme [16] to implement the discrete Laplace-Beltrami operator. The COT scheme is based on discretization of the heat equation and is observed to produce eigenfunctions that approximately preserve the convergence property of the continuous Laplace operator for a reasonably well sampled triangular mesh [5]. We also show how the detected symmetries can be further analyzed for symmetry characterization and clustering, potentially revealing greater semantic information about the underlying 3D shape.

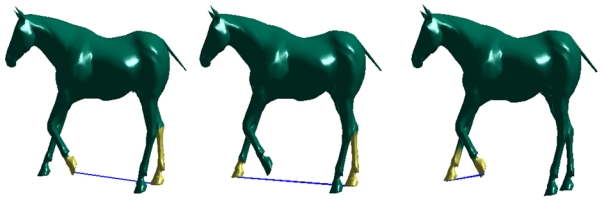

Fig. 4. Examples of overlapping symmetry detection for the *Horse* shape model.

### A. Symmetry Detection

The results of the proposed symmetry detection algorithm are depicted in Figs. 2 and 4. Several important properties of the proposed algorithm are highlighted in these results.

*1) General Symmetry Detection:* The ability of the proposed algorithm to identify multiple intrinsic symmetries is evident from the results shown in Fig. 4. The extracted symmetries are seen to cover the global symmetry of the underlying 3D shape which has undergone approximately isometric deformations. Additionally, the proposed algorithm is also observed to be capable of detecting symmetry transformations that cover individual components of a 3D object that possess various forms of self-symmetry.

*2) Overlapping Symmetry Detection:* An important aspect of the proposed algorithm is its ability to detect instances of overlapping symmetry. An instance of overlapping symmetry is deemed to occur when a specific region on the surface of the 3D shape is simultaneously subjected to more than one symmetry transformation and hence is symmetric to more than one region on the 3D shape surface. Fig. 4 shows examples of successful detection of overlapping symmetry between the legs of the *Horse* shape model by the proposed algorithm. Three different combinations of the detected overlapping symmetry transformations between the four legs of the *Horse* model (out of a total of six possibilities) are depicted in Fig. 4.

### B. Performance Statistics

The experiments reported in this paper were performed on an Intel Core$^{TM}$ 3.4 GHz machine with 24 GB RAM. Table I reports the timing results for the various steps of the proposed symmetry detection algorithm. The most time consuming step, i.e., the all-pairs biharmonic distance computation, accounts for $\approx 80\%$ of the execution time of the proposed algorithm. More importantly, bypassing the two-step spectral clustering procedure described in [23] reduces significantly the computation time of the proposed algorithm.

### C. Comparisons

We compare the proposed symmetry detection algorithm with two sufficiently similar methods [9], [23]. Though both methods [9], [23] are capable of *detecting* instances of partial intrinsic symmetry, neither is able to *characterize* the underlying symmetry. In contrast, the proposed algorithm, not only detects overlapping intrinsic symmetries, but it also has the ability to characterize and cluster the detected symmetries in symmetry space. In the proposed algorithm, interpolation of the functional map of symmetry transformations from the chosen point pair to the remaining point pairs (i.e., identification of other point correspondences from those obtained via the CSV procedure) is achieved by solving a system of linear equations which is computationally much more efficient than the two-stage spectral clustering procedure of Xu et al [23]. In contrast to the proposed algorithm, the symmetry-factored embedding (SFE) technique of Lipman et al. [9] is incapable of detecting cases of overlapping intrinsic symmetries resulting in poor symmetry-based segmentation of the 3D shape (Fig. 5).

TABLE I

TIMING RESULTS FOR THE VARIOUS STEPS IN THE PROPOSED ALGORITHM. BIHARMONIC: TIME TAKEN TO COMPUTE THE ALL-PAIRS BIHARMONIC DISTANCE; FMAP: TIME TAKEN TO COMPUTE THE FUNCTIONAL MAPS; EXTRACTION: TIME TAKEN FOR SYMMETRY EXTRACTION; TOTAL: TOTAL EXECUTION TIME. ALL TIMES ARE MEASURED IN SECONDS.

| # Points | Biharmonic | FMap | Extraction | Total |
|---|---|---|---|---|
| 3400 | 32 | 2 | 5 | 39 |
| 10000 | 41 | 3 | 7 | 51 |
| 50000 | 237 | 4 | 15 | 256 |

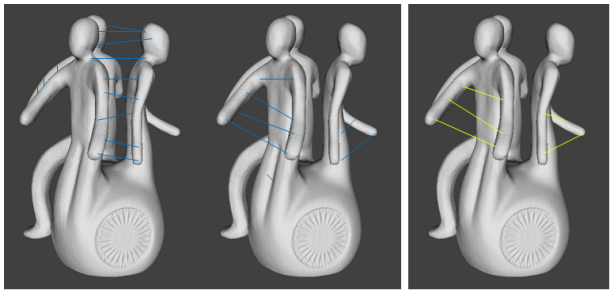


Fig. 5. The proposed CSV procedure ensures detection of instances of global overlapping intrinsic symmetry (a), (b). In contrast, Lipman et al. [9] fails to detect instances of overlapping symmetry (c).

### D. Performance in Presence of Noise

The proposed symmetry extraction algorithm is evaluated on the TOSCA dataset [3] under varying levels of additive white Gaussian noise. The mean normalized error (MNE) in the functional map is computed over all the point correspondences for varying $\sigma$ values of the white Gaussian noise (Fig. 6). It is interesting to note that the MNE initially increases with increasing values of $\sigma$ before settling upon a value of $\approx 0.0007$ for values of $\sigma > 0.4$, thus depicting the robustness of proposed technique to additive white Gaussian noise.

### E. Quantitative Evaluation

We used the SHREC 2010 feature detection and description benchmark [4] to evaluate the proposed algorithm. We considered shapes that have undergone perturbations characterized by isometry, topology, micro-holes, scale and noise. The quantitative evaluation is along the lines proposed by Sipiran and Bustos [21] and its goal is to determine whether the extracted symmetric components are consistent between a null shape $X$ and the transformed shape $Y$ where the

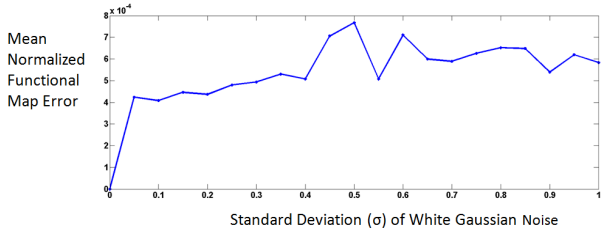


Fig. 6. Normalized error in the functional map for varying levels of additive white Gaussian noise.

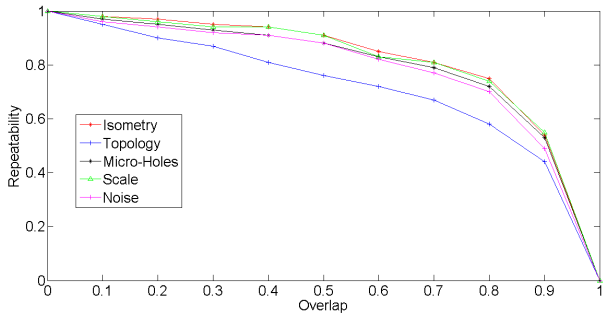


Fig. 7. Plot of repeatability vs. overlap for the proposed symmetry detection algorithm on the SHREC 2010 benchmark dataset.

extracted symmetric components are $S_X = \{X_1, \ldots, X_n\}$ and $S_Y = \{Y_1, \ldots, Y_m\}$, respectively. Using the ground-truth data, we compute for each component $Y_j \in S_Y$ the corresponding component $X'_j$ in $S_X$. The component repeatability between $X$ and $Y$ is defined as: $R(X,Y) = \sum_{j=1}^{m} \max_{1 \le i \le n} O(X_i, X'_j)$ where, the overlap $O(X_i, X'_j)$ between two extracted symmetric components $X_i$ and $X'_j$ is defined as: $O(X_i, X'_j) = \dfrac{A(X_i \cap X'_j)}{A(X_i \cup X'_j)}$ where $A(X)$ is the surface area of component $X$. The repeatability $R$ in overlap $O$ is defined as the fraction of symmetric components in $S_Y$ that have an overlap greater than $O$ with their corresponding components in $S_X$ [21]. A resilient symmetry extraction algorithm is expected to exhibit high values of $R$ ($\approx 1$) for a wide range of $O$ values. Fig. 7 shows the plot of $R$ versus $O$ for various surface perturbations. The proposed symmetry extraction algorithm is seen to maintain a high overall repeatability $R \geq 0.80$ at overlap values $O \leq 0.75$ for most surface perturbations.

### F. Symmetry Characterization

The degree of diagonality of the functional map $C$ could be used to characterize the complexity of the underlying symmetry transformation. The more complex the symmetry transformation, the greater the deviation of the shape deformation from intrinsic isometry. This results in a deformation characterized by a functional matrix $C$ with higher off-diagonal element values and a higher value for the inner product of $C$ and the weight matrix $W$. The resulting characterization of the isometric deformation is depicted in Fig. 3.

## VI. Conclusions and Future Directions

We have presented an algorithm for detection and characterization of intrinsic symmetry in 3D shapes. Our algorithm attempts to formalize the symmetry analysis problem, not only as one of symmetry detection, but as one that includes symmetry characterization in the transformation space. In particular, the introduction of the functional map formalism in symmetry detection enables us to come up with a novel representation of the symmetry transformation as a functional map. In the near future, we aim to formulate operations, such as addition and subtraction, on these generated functional maps that would potentially provide a deeper and more comprehensive understanding of intrinsic symmetry in general. We also plan to study the possibility of transformation map-based exploration of symmetry transformations across non-isometric deformable shapes.

## References


[1] Aubry et al. (2011) The wave kernel signature: A quantum mechanical approach to shape analysis. *Proc. Comp. Vis. Wrkshps. (ICCV Wrkshps)*.

[2] Bronstein et al. (2007) Calculus of non-rigid surfaces for geometry and texture manipulation. *IEEE Trans. Visualization & Computer Graphics*, Vol 13(5), September-October, pp. 902–913.

[3] Bronstein et al. (2008) *Numerical Geometry of Non-rigid Shapes*. Springer, 2008. ISBN: 978-0-387-73300-5.

[4] Bronstein et al. (2010) SHREC 2010: Robust feature detection and description benchmark. *Proc. Wkshp. 3D Object Retrieval (3DOR10)*.

[5] Belkin et al. (2008) Discrete Laplace operator on meshed surface. *Proc. Symp. Comp. Geometry*, pp. 278–287.

[6] Eldar et al. (1997). The farthest point strategy for progressive image sampling. *IEEE Trans. Image Processing*, 6(9) pp. 1305–1315.

[7] Kazdhan et al., (2003) A reflective symmetry descriptor for 3D models. *Algorithmica*, 38(1), October, pp. 201–225.

[8] Li et al., (2005) Fast global reflectional symmetry detection for robotic grasping and visual tracking. *Proc. Australasian Conf. Robotics and Automation (ACRA05)*, December.

[9] Lipman et al. (2010). Symmetry factored embedding and distance. *ACM Trans. Graphics (TOG)*, 29(4) pp. 103.

[10] Lipman et al. (2010). Biharmonic distance. *ACM Trans. Graphics (TOG)*, 29(3) pp. 27.

[11] Mitra et al. (2006) Partial and approximate symmetry detection for 3D geometry. *ACM Trans. Graphics (TOG)*, 25(3) pp. 560–568.

[12] Mitra et al. (2013) Symmetry in 3D geometry: Extraction and applications. *Comp. Graphics Forum*, 32(6) pp. 1–23.

[13] Ovsjanikov et al. (2008) Global intrinsic symmetries of shapes. *Comp. Graphics Forum* 27(5) pp. 1341–1348.

[14] Ovsjanikov et al. (2010) One point isometric matching with the heat kernel. *Comp. Graphics Forum*, 29(5) pp. 1555-1564.

[15] Ovsjanikov et al. (2012) Functional maps: A flexible representation of maps between shapes. *ACM Trans. Graphics (TOG)*, 31(4) pp. 30.1–30.11.

[16] Pinkall and Polthier (1993) Computing discrete minimal surfaces and their conjugates. *Experimental Mathematics*, 2(1) pp. 15–36.

[17] Podolak et al. (2006) A planar-reflective symmetry transform for 3D shapes. *ACM Trans. Graphics (TOG)* 25(3), July, pp. 549–559.

[18] Pokrass et al. (2013) Sparse modeling of intrinsic correspondences. *Comp. Graphics Forum*, 32(2) pp. 459–468.

[19] Raviv et al. (2007) Symmetries of non-rigid shapes. *Proc. Intl. Conf. Computer Vision*, pp. 1–7.

[20] Raviv et al. (2010) Full and partial symmetries of non-rigid shapes. *Intl. Jour. Computer Vision* 89(1), pp. 18-39.

[21] Sipiran and Bustos (2012) Key-component detection on 3D meshes using local features. *Proc. Eurographics Conf. 3D Object Retrieval*, pp. 25–32.

[22] Xu et al., (2009) Partial intrinsic reflectional symmetry of 3D shapes. *ACM Trans. Graphics (TOG)*, 28(5), pp. 138:1-10.

[23] Xu et al. (2012) Multi-scale partial intrinsic symmetry detection. *ACM Trans. Graphics (TOG)*, 31(6), pp. 181.

[24] Yen et al. (2007) Graph nodes clustering based on the commute-time kernel. *Proc. Pcfc-Asia Conf. Know. Discv. Data Mining (PAKDD 2007)*.

[25] Zabrodsky et al., (1995) Symmetry as a Continuous Feature, *IEEE Trans. Pattern Anal. & Mach. Intell.*, 17(12), pp. 1154–116.